

RSC Advances



This is an *Accepted Manuscript*, which has been through the Royal Society of Chemistry peer review process and has been accepted for publication.

Accepted Manuscripts are published online shortly after acceptance, before technical editing, formatting and proof reading. Using this free service, authors can make their results available to the community, in citable form, before we publish the edited article. This *Accepted Manuscript* will be replaced by the edited, formatted and paginated article as soon as this is available.

You can find more information about *Accepted Manuscripts* in the [Information for Authors](#).

Please note that technical editing may introduce minor changes to the text and/or graphics, which may alter content. The journal's standard [Terms & Conditions](#) and the [Ethical guidelines](#) still apply. In no event shall the Royal Society of Chemistry be held responsible for any errors or omissions in this *Accepted Manuscript* or any consequences arising from the use of any information it contains.

A cost-effective disposable graphene-modified electrode decorated with alternating layers of Au NPs for the simultaneous detection of dopamine and uric acid in human urine

Nadeem Baig and Abdel-Nasser Kawde*

Chemistry Department, King Fahd University of Petroleum and Minerals, Dhahran 31261, Saudi Arabia

*Corresponding Author, e-mail: akawde@kfupm.edu.sa

Abstract:

A disposable electrode based on a highly sensitive and readily fabricated arrangement of alternating AuNP and graphene layers was introduced for the simultaneous determination of dopamine and uric acid. The process by which the disposable electrodes were fabricated is simple, fast, and accomplished through the direct electrochemical reduction of graphene oxide and Au (III) onto a graphite pencil electrode surface. Extraordinary electrocatalytic activities of the graphene nanocomposite were observed in the presence of dopamine and uric acid. The synthesized graphene oxide was characterized by Raman and FTIR spectroscopy. The surface morphology, elemental, and electrochemical characterization of the bare and modified electrodes were analyzed by field emission scanning electron microscopy (FE-SEM), energy dispersive X-ray spectroscopy (EDX), cyclic voltammetry (CV), and electrochemical impedance spectroscopy (EIS). Good linear sensitivity was obtained over the ranges of 0.1–25 μM for dopamine and 0.09–25 μM for uric acid under optimal conditions using square wave voltammetry. Very low limits of detection of 0.024 μM (dopamine) and 0.029 μM (uric acid) were attained from the fabricated electrochemical sensors. The dopamine and uric acid peak separation was 151 mV. The graphene nanocomposite on the GPE surface effectively improved the peak separation, electroactive surface area, sensitivity, selectivity, and reproducibility. The fabricated electrode behaved well in the presence of high concentrations of ascorbic acid and in the presence of other potentially interfering compounds. The electrochemical sensors did not undergo surface fouling, particularly in the presence of dopamine, which tends to severely foul surfaces after a single measurement. The cost effectiveness of the sensor, the short fabrication time, and the lack of surface fouling, especially in the presence of dopamine, render these novel electrodes both multi-use and disposable.

Keywords: Dopamine, uric acid, gold nanoparticles, graphene, disposable GPE, Urine

Introduction:

Dopamine and uric acid are crucial biomolecules that normally co-occur in physiological fluids such as urine and serum.¹ Abnormal levels of dopamine and uric acid in the body could lead to numerous fatal diseases. The simultaneous detection of dopamine and uric acid is critical to characterizing the health condition of an individual. Dopamine belongs to the catecholamine family and acts as a vital neurotransmitter in the central nervous system.^{2,3} Dopamine also plays a major role in the hormonal and cardiovascular systems.⁴ Abnormal dopamine levels in the body could cause serious conditions, including Parkinson's disease, schizophrenia, restless leg syndrome (RLS), and attention deficit hyperactivity disorder.⁵ Uric acid is an important biomarker and is produced in the body by purine metabolism.⁶ Abnormal levels of uric acid in the body could cause gout, hyperuricemia, and Lesch–Nyhan syndrome.⁷ The extraordinary importance of dopamine and uric acid in the body underscores the importance of developing sensitive and reliable methods for their detection.

Several sensitive dopamine and uric acid detection approaches have been developed. Electrochemical methods are attractive over alternative methods due to their sensitivity, selectivity, rapid sensing capabilities, simple operation, and low cost.⁸ The individual or simultaneous detection of dopamine and uric acid using conventional electrodes has been difficult due to their electrochemical oxidation poor kinetics and overlapping oxidation potentials.⁹ Conventional electrodes could not be used directly for the simultaneous detection of dopamine and uric acid. The selectivity and sensitivity of the bare electrode surfaces may be improved using a variety of methods to overcome the overlapping oxidation potentials of dopamine and uric acid.¹⁰ The literature describes the use of several modified and complex materials for the simultaneous detection of dopamine and uric acid. Modified electrodes, such as NiCo-NPs-in-N/C modified GCE^a,¹¹ PL-LEU/DNA/GCE^a,¹² ZnO–Cu_xO–PPy/GCE^a,¹³ NiCo₂O₄/Nano-ZSM-5/GCE^a,¹⁴ and GNPs/PI_{ox}/GCE^a,¹⁵ have been used for simultaneous detection.

Graphene has recently attracted attention for its extraordinary mechanical strength, high surface area, and electrical and thermal conductivity.¹⁶ The interesting properties of graphene have inspired widespread exploration in the field of transparent conductors, energy storage devices, field emission displays, and chemical and biological sensing.¹⁷ Graphene is potentially useful for

the fabrication of electrochemical sensors due to its engagement in rapid electron transfer, its small charge transfer resistance, its large potential window, and its huge electroactive surface area.¹⁸ Graphene-based sensors, including CTAB/rGO/ZnS/GCE^a,¹⁹ CTAB-GO/MWNT/GCE^a,²⁰ and Pd₃Pt₁/PDDA-RGO/GCE^a, have been introduced for the simultaneous detection of dopamine and uric acid. The electrocatalytic activity, biocompatibility, and excellent conductivity²¹ of Au NPs has been combined with graphene to enhance the sensitivity and selectivity of electrodes. Previously studies of layered graphene and Au NP assemblies (GE/Au/GE/CFE) have fabricated these assemblies on carbon fiber electrodes. The sensitivity of this electrode was not very good. The limits of detection obtained from the GE/Au/GE/CFE^a assembly were 0.59 μM for dopamine and 12.6 μM for uric acid.²² Wang et al.⁸ fabricated an Au/RGO/GCE^a to improve the sensitivity to uric acid detection (1.8 μM), although this electrode's response to dopamine remained poor (1.4 μM). The uric acid–dopamine peak separation was 110 mV, less than that reported elsewhere. None of the aforementioned electrodes were disposable in the context of dopamine and uric acid sensing. In most cases, complex steps were involved in fabricating the sensitive electrodes, and rendering the surfaces reusable remained a significant challenge. Dopamine easily fouled the surface, even after a single measurement. Regenerating the surface for a second measurement proved to be difficult.

In this work, we fabricated a disposable graphene nanocomposite electrode. Alternating Au NP and graphene layers were formed on a GPE surface through the direct electrochemical reduction of Au(III) or graphene oxide solutions. The fabrication of this arrangement provided a good electroactive surface area for the electrochemical reaction and was more facile and rapid compared to the casting methods commonly used to modify electrodes. We obtained significant peak separation and a low limit of detection compared to previous studies of Au and graphene for the simultaneous detection of dopamine and uric acid. After each sensing measurement, the electrode surface could be renewed. To the best of our knowledge, this work constitutes the first attempt at fabricating a disposable electrode based on alternating Au NP and graphene layers on a GPE surface for the simultaneous detection of dopamine and uric acid. A low-cost single-use electrode, such as the GPE, provides a good alternate to the widely used glassy carbon electrode (GCE) and carbon paste electrode (CPE).

Materials and methods:

Reagents:

Dopamine, H₂O₂, uric acid, fructose, l-methionine, acetate buffer, potassium chloride, sodium chloride, Hydrogen tetrachlorocuprate(III)hydrate was purchased from Sigma-Aldrich (USA). Phenylalanine and alanine were received from Fluka (USA). Sodium phosphate monobasic, di-Potassium hydrogen orthophosphate and potassium permanganate (KMnO₄) were obtained from BDH (England). Double distilled water was obtained from laboratory-based Water Still Aquatron A 4000 D (UK) and was used for the preparation of different solutions and in the entire experimental work.

Apparatus:

The electrochemical impedance spectroscopy and the voltammetric experiments were executed by using a potentiostat Auto Lab (Netherland). Three-electrode system was used for voltammetric measurement which consists of Ag/AgCl reference electrode, the counter electrode was platinum (Pt) and working electrodes were bare GPE, Au/GPE, GR/GPE or GR/Au/GR/Au/GPE. The 7 mm pencil was extruded from the vertically fixed pencil holder and was dipped in the solution for the modification and all experimental measurements. The aspects of the graphite pencil electrode have described previously in detail.²³ The EDX spectra and FE-SEM images were collected for the bare and the modified electrode surfaces using TESCAN LYRA 3 (Brno, Czech Republic) at the Center of Research Excellence in Nanotechnology, KFUPM. FTIR or Raman spectra of graphite and graphene oxide were scanned by NICOLET 6700 FT-IR and HORIBA Scientific LabRAM HR Evolution, respectively. The weight of different compounds and the pH of the buffers were controlled by GR-2000 electrical balance and Accumet® XL50 pH meter.

Fabrication of GR/Au/GR/Au/GPE sensor:

The optimized conditions for the modification material were used for the fabrication of the electrode for the simultaneous detection of dopamine and uric acid. The graphene oxide modification conditions were already discussed in detail.²⁴ The 0.5 mM HAuCl₄ was prepared in

0.1M KNO₃ solution. The graphene oxide (4 mg/mL) was dispersed by sonicating in 0.1 M acetate buffer. The alternative layers of Au NPs were formed on the GPE surface by the electrochemical reduction of Au (III) by cyclic potential swept from -0.4 to 0.3 V at scan rate of 10 mV over 1 cycle. After each Au NPs layer, the graphene layer was formed by the electrochemical reduction of graphene oxide by cyclic potential sweeping from -1.4 to 0.3 V over 1 cycle. After every layer, the modified electrode was washed gently three times by simply dipping in the double distilled water. The modified electrode was represented as GR/Au/GR/Au/GPE.

Live subject statement

All experiments were performed in compliance with the relevant laws and institutional guidelines. A consent was obtained for any experimentation with human subjects.

Results and discussion:

Characterization of the synthesized graphene oxide:

The synthesized graphene oxide was characterized by Raman and FTIR spectrometry. Strong D and G bands in the GO Raman spectra were observed at 1344 cm⁻¹ and 1590 cm⁻¹, respectively. The 2D band, considered to be the overtone of the D band, appeared at 2691 cm⁻¹ (Fig. 1Ab). The D band corresponded to structural defects, and the G band corresponded to first-order scattering from the E_{2g} phonon. A weak D band was observed for the graphite Raman spectra (Fig. 1Aa). FTIR spectra characteristic of graphene oxide and graphite confirmed the formation of graphene oxide from graphite (Fig. 1B). The prominent and broad stretching vibrational absorption peak corresponding to the -OH group appeared at 3425 cm⁻¹. The absorption peaks at 1733 cm⁻¹ and 1625 cm⁻¹ were assigned to carboxylic acid C=O and aromatic -C=C- groups, respectively. -C-O stretching vibrations were observed for the carboxylic acid, epoxy, and alkoxy functional groups at 1383 cm⁻¹, 1225 cm⁻¹, and 1050 cm⁻¹, respectively.²⁴

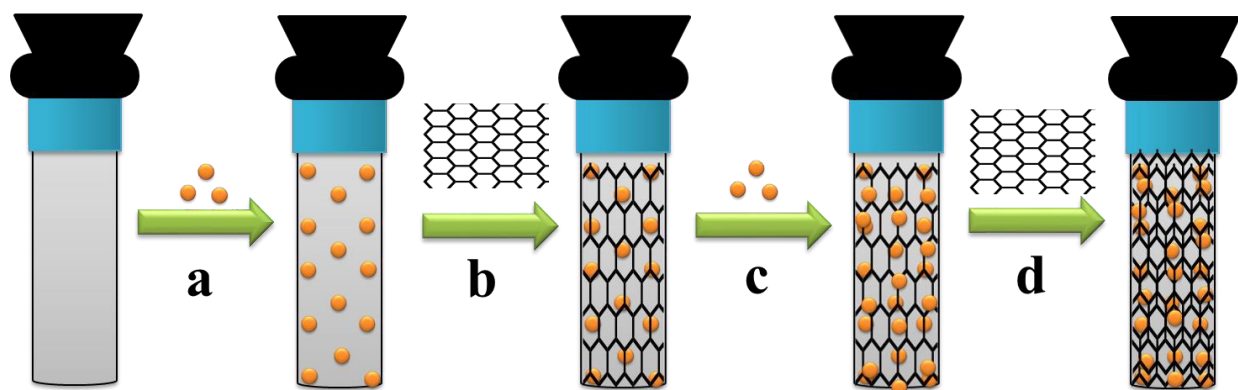
Optimization of the conditions for fabrication a sensitive sensor

The sensitivity of the electrode was enhanced by optimizing the graphene and Au NP fabrication conditions from graphene oxide and HAuCl₄, respectively. The optimal graphene conditions for

preparing the GPE have been reported previously.²⁴ The concentration of HAuCl₄ was optimized over the range 0.05 mM to 0.15 mM. A maximum response was obtained at 0.5 mM (Fig. S1). The optimal scan rate for the electrochemical reduction of Au⁺³ onto the GPE surface to form Au NPs was found to be 0.01 V/s (Fig. S2). Different scan windows were analyzed, and a better response to dopamine and uric acid was observed using a CV scan window of -0.4 to 0.3 V for Au NPs formation on the electrode surface (Fig. S3). A variety of electrolytes were analyzed, and KNO₃ was found to be effective for the incorporation of Au NPs onto the electrode surface (Fig. S4).

Combination of Au NPs and graphene layers patterned onto the electrode surface, and stepwise morphological characterization of the sensing surface

The layer arrangements on the GPE surface were characterized by miniaturizing a variety of Au NPs and graphene patterns on the GPE surface. CV scans were collected in the presence of a 0.2 mM dopamine and uric acid solution in 0.1 M PBS using different electrodes with a variety of layer combinations. An analysis of the different layers revealed that the sensor was more efficient for the simultaneous detection of dopamine and uric acid if graphene comprised the outer layer and the Au NPs formed an inner layer on the electrode surface. Two combinations were found to provide the best responses: a sandwich scheme, in which the Au NPs formed an inner layer and the graphene formed an outer layer, GR/Au/GR/GPE (Fig. 2B), and alternating Au and graphene layers, in which the Au NPs were deposited as the first layer, GR/Au/GR/Au/GPE (Fig. 2A). The GR/Au/GR/Au/GPE was selected for further study due to its slightly better response compared to GR/Au/GR/GPE. The various steps involved in fabricating the sensitive electrodes for the simultaneous measurement of dopamine and uric acid are presented in Scheme 1. The greater efficiency of the sensors fabricated with an outer graphene layer may have resulted from attractive forces between graphene and the dopamine and uric acid molecules.



Scheme 1 Schematic representation of the stepwise fabrication of modified electrode: the electrochemical formation of Au NPs on GPE (a), formation of graphene layer on Au/GPE (b), second layer of Au on GR/Au/GPE (c), and outer layer of GR on Au/GR/Au/GPE (d).

The surface morphologies during GPE layer formation surface were analyzed in a stepwise fashion using field emission scanning electron microscopy. The graphene-modified electrode was fabricated on the GPE surface by reducing GO (4 mg/mL) under two cyclic voltammetry scans from -1.4 to 0.3 V. The SEM images clearly revealed the formation of wrinkle-shaped graphene layers on the GPE surface (Fig. 3b). No such layers were present on the bare GPE surface (Fig. 3a). Stepwise SEM images of the surface were compared to reveal the morphological changes after each step fabrication process.

The first layer of Au NPs was deposited onto the GPE surface using a CV scan between -0.4 and 0.3 V over 1 cycle. Well-distributed Au NPs were observed in the SEM image (Fig. 4a). In the second electrode modification step, the graphene layer was formed by reducing GO, and the SEM images clearly revealed the presence of Au NPs beneath the graphene layer (Fig. 4b). The second Au NPs layer was embedded in the first graphene layer (Fig. 4c). Finally, the wrinkled and crumpled shape of the second graphene layer was formed by GO reduction (Fig. 4d). The presence of Au NPs on the surface of the final modified electrode was confirmed by energy dispersive X-ray spectroscopy mapping. The spectrum confirmed the presence of Au on the GPE surface (Fig. 5).

Electrochemical and kinetics study of the modified electrode

The CV scan rate effects were examined for the bare, GR/GPE, and GR/Au/GR/Au/GPE in the presence of a 5 mM $\text{K}_3\text{Fe}(\text{CN})_6/\text{K}_4\text{Fe}(\text{CN})_6$ solution in 0.1 M KCl. The scan rate was varied over the range 20 mVs^{-1} to 100 mVs^{-1} for the $\text{K}_3\text{Fe}(\text{CN})_6/\text{K}_4\text{Fe}(\text{CN})_6$ solution (Fig. S5, A, B and C) and over the range 50 mVs^{-1} to 350 mVs^{-1} for the 0.2 mM uric acid and 1 mM dopamine solution (Fig. S6). The current increased as the scan rate increased. A linear relationship was observed between the square root of the scan rate and the peak current. At higher scan rates, the response of the bare electrode was not good compared to the modified electrodes. This result suggested that higher scan rates required the electrochemical reaction to reach completion in a shorter period of time, and the bare electrode surface could not support the fast charge transfer as well as the modified electrodes. The electroactive surface area was calculated for the bare, GR/GPE, and GR/Au/GR/Au/GPE electrodes using the Randles–Sevcik equation

$$I_p = 2.69 \times 10^5 \gamma^{1/2} D^{1/2} n^{3/2} C A, \quad 1$$

where I_p is the peak current (A), γ is the scan rate (Vs^{-1}), D is the diffusion coefficient ($\text{cm}^2 \text{ s}^{-1}$), n is the number of electrons, C is the concentration of the analyte (mol L^{-1}), and A is the electroactive surface area of the electrode (cm^2). The electroactive surface area was calculated using a 5 mM $\text{K}_3\text{Fe}(\text{CN})_6/\text{K}_4\text{Fe}(\text{CN})_6$ solution in 0.1 M KCl for the bare, GR/GPE, and GR/Au/GR/Au/GPE. The graphene layer was found to be very effective at increasing the electroactive surface area. The electroactive surface area was further improved by the graphene and Au NPs layer arrangement on the GPE surface. The electroactive surface areas were 0.066 cm^2 , 0.376 cm^2 , and 0.518 cm^2 for the bare, GR/GPE, and GR/Au/GR/Au/GPE, respectively. The electroactive surface areas of the modified electrodes were also calculated for the 0.2 mM uric acid and 1 mM dopamine solutions in 0.1 M PBS buffer. The electroactive surface areas obtained for uric acid were 0.948 cm^2 and 1.21 cm^2 , and those obtained for dopamine were 0.668 cm^2 and 0.7718 cm^2 on GR/GPE and GR/Au/GR/Au/GPE, respectively (Fig. S6). The surface area study revealed that graphene efficiently increased the surface area, which was further improved by the alternating layers of graphene and Au NPs on the electrode surface.

The interfacial characteristics of the bare and the modified electrodes were further characterized by electrochemical impedance spectroscopy. Figure S5, D presents the EIS spectra of the bare GPE, Au/GPE, GR/GPE, and GR/Au/GR/Au/GPE. A large semicircle was observed in the case of the bare GPE. The large semicircle indicated a high interfacial resistance of approximately

2500 Ω . The Au NPs on the GPE surface effectively reduced the interfacial resistance to 18 Ω . The low resistance of the Au NPs significantly improved the conductance of the GPE. The graphene and Au NPs combination yielded a fairly straight line in the EIS spectrum. The same was observed for the graphene-modified electrode, indicating that the graphene–Au NPs combination nearly overcame the charge transfer resistance.

The electrochemical properties of the various pencil graphite electrode surfaces were further investigated by recording the cyclic voltammograms in the presence of 0.5 mM dopamine and uric acid solutions in 0.1 M PBS. The response of the bare surface (Fig. 6a) during simultaneous detection was not sensitive at all. The dopamine and uric acid peak separation was very poor and insufficient for use in simultaneous sensing. The Au NPs on the GPE surface improved the sensitivity and peak separation slightly (Fig. 6b). The graphene layers (Fig. 6c) provided significantly better peak separation and sensitivity. Furthermore, the alternating arrangements of Au NPs and graphene layers (Fig. 6d) considerably enhanced the current compared to the bare GPE, Au NPs/GPE, and GR/GPE.

The electrode surface played a vital role in controlling the kinetics and reversibility of the electrochemical reactions.²⁵ The reversibility of the electrochemical reaction was investigated by cyclic voltammetry. The potential difference of the reversible reaction is expressed by equation 2.

$$\Delta E = E_{pa} - E_{pc} = 59/n, \quad 2$$

where ΔE (mV) is the peak potential difference between the anodic and cathodic peak potentials, E_{pa} (mV) is the anodic peak potential, E_{pc} (mV) is the cathodic peak potential and n is the number of electrons taking part in the electrochemical reaction. An irreversible reaction yields only a single peak. The electrochemical reaction was reversible if the value of ΔE was 59/n mV and was quasi-reversible for a value exceeding 59/n mV. The ΔE values calculated using equation 2 were 31.0 mV for uric acid and 39.8 mV for dopamine. The calculated values of ΔE for dopamine and uric acid exceeded $2.3RT/nF$ or 59/n mV, indicating that the electrochemical reactions of dopamine and uric acid were quasi-reversible on the modified electrode surface. The values of n (number of electrons) for dopamine and uric acid were calculated (Eq. 2) to be 1.5 and 1.9, respectively. The experimental values of n indicated the involvement of two electrons in the electrochemical reactions of dopamine and uric acid on the GR/Au/GR/Au/GPE surfaces.

Study of pH

The effects of the PBS solution pH on the dopamine and uric acid detection were explored. The pH influence was investigated by varying the pH of the 0.1 M PBS solution from 5.0 to 7.5 in the presence of 0.5 mM dopamine and uric acid. The cyclic voltammograms obtained from the simultaneous measurements of dopamine and uric acid revealed the impact of pH on the current and on the oxidation and reduction peak potentials. The optimum response was obtained at a pH of 6.0. A negative peak shift was observed during the dopamine and uric measurements as the pH increased (Fig. S7). The negative shift with increasing pH indicated the direct involvement of protons in the oxidation of the uric acid and dopamine. A linear relationship was observed between the peak shift potential and the pH of the medium for uric acid ($R^2 = 0.988$) and dopamine ($R^2 = 0.991$). The slope was found to be 51.3 mV/pH for uric acid (Eq. 3) and 50.6 mV/pH for dopamine (Eq. 4), in good agreement with the theoretical value of 59 mV/pH. These values for the slope revealed that equal numbers of protons and electrons were involved in the electrooxidation of dopamine and uric acid. The transfer of two electrons and the mean involvement of two protons in the electrochemical reaction were calculated using Equation 2.

$$E \text{ vs. Ag/AgCl} = -0.0513 [\text{pH}] + 0.6991 \quad 3$$

$$E \text{ vs. Ag/AgCl} = -0.0506 [\text{pH}] + 0.5261 \quad 4$$

Optimization of the SWV

Different voltammetric techniques were applied for dopamine and uric acid detection. The SWV was found to be much more sensitive than the other techniques for dopamine and uric acid detection. The electrode sensitivity toward the analyte could be enhanced by optimizing the SWV parameters. The amplitude displayed different effects on the dopamine and uric acid detection. The oxidation peak currents of both analytes increased as the amplitude increased to 0.04 V. The current subsequently decreased dramatically as the amplitude was increased in the presence of uric acid, whereas the current continued to increase in the presence of dopamine and then decreased beyond 0.06 V (Fig. S8, A). The frequency was also found to impact the peak current. The maximum responses for dopamine and uric acid were observed at 50 Hz, and the current dropped at higher frequencies (Fig. S8, B). The GR/Au/GR/Au/GPE electrode displayed excellent adsorption properties for dopamine and uric acid. The adsorption properties were

improved by the presence of the graphene layer on the electrode surface. The π electron-rich system and the large surface area of the graphene enhanced the adsorption of the analyte,²⁶ as indicated by the sharp rise in the current as the adsorption time increased. The surface of the modified electrode became saturated at 120 s (Fig. S8, C).

The simultaneous detection of dopamine and uric acid, reproducibility, and the detection limit

The responses of the electrodes to dopamine and uric acid at the GR/Au/GR/Au/GPE surface were measured in the presence of various analyte concentrations. Well-resolved dopamine and uric acid peaks were observed at 0.232 V and 0.383 V, respectively. The peak separation between dopamine and uric acid was 0.151 V. Linear responses during the simultaneous detection were attained for the concentration ranges 0.1 μ M and 25 μ M dopamine and 0.09 μ M to 25 μ M uric acid (Fig. 7A). The limits of detection ($S/N = 3$) for dopamine and uric acid were 0.024 and 0.029 μ M, respectively. The detection and quantification limits achieved at the fabricated electrode were much better or comparable to the corresponding limits reported previously for graphene and graphene nanocomposite electrodes. The response of each analyte was considered while holding the other analyte concentrations constant (Fig. 7, B and C).

The fabrication reproducibility was checked by fabricating five different GR/Au/GR/Au/GPEs under the same set of conditions. The RSD ($n = 5$) values for the simultaneous detection of dopamine and uric acid were found to be 7.56% and 3.07%, respectively.

Comparison with previously described graphene composites and, particularly, with Au NP graphene composites

The simultaneous detection of dopamine and uric acid was challenging, and several methods were introduced to improve the sensitivity of detection. A few literature reports have described the use of Au–graphene composites for this purpose. The GE/Au/GE layer arrangement was previously fabricated on a carbon fiber electrode. The limits of detection obtained using this electrode (0.59 for dopamine and 12.6 μ M for uric acid) indicated that the arrangement was not very sensitive toward the analytes²². Another study examined a glassy carbon electrode modified with reduced graphene oxide and electrodeposited gold nanoplates, which yielded an LOD of 1.4 for dopamine and 1.8 μ M for uric acid. The dopamine–uric acid peak separation was 110 mV.⁸ A

combination of Au NPs, β cyclodextrin, and graphene was used in another study to enhance the sensitivity of the GCE. The detection limits were significantly improved to 0.15 μM (dopamine) and 0.21 μM (uric acid), and the peak separation was increased to 120 mV.²¹ Other graphene nanocomposites have been reported for the simultaneous detection of dopamine and uric acid, as listed in Table 1. In the present work, we found that the direct reduction of graphene oxide and Au(III) onto a disposable graphite pencil electrode surface was highly effective for the simultaneous sensing of dopamine and uric acid. The limit of detection was dramatically improved to 0.024 (dopamine) and 0.029 μM (uric acid) compared to previous studies, particularly compared to previous graphene–Au nanocomposite electrodes. The fabricated electrode is disposable and highly cost-effective, the modification method is facile compared the casting methods, which can require hours to obtain a dry electrode surface and further electrochemical treatments to enable the use of these electrode surfaces in sensing applications.

Actual sample and interference studies

The fabricated GR/Au/GR/Au/GPE was used to detect dopamine and uric acid in a urine sample collected from a healthy person. The concentration of uric acid in urine is high; therefore, the sample was diluted to bring the value into the linear detection range of the fabricated electrode. The urine sample was not treated in any other way prior to conducting the measurements. The dopamine and uric acid concentrations were obtained using standard addition methods. The urine samples were spiked with 2, 4, or 8 μM dopamine and uric acid. Recoveries in the range of 93–109% were obtained (Table 2). The RSD ($n = 3$) values were less than 8.1%. The modified electrode detection properties were examined for potential interference from other urine components. Good recoveries of the dopamine and uric acid concentrations in the urine sample indicated that the electrode efficiently coped with interference from other substances present in the actual urine sample. The biomolecule that interfered the most with the simultaneous measurements of dopamine and uric acid was ascorbic acid. Dopamine and uric acid measurements were obtained in the presence of 1 mM ascorbic acid, and current variations of 7.0% for dopamine and 9.3% for uric acid were obtained. The presence of 0.1 mM fructose,

alanine, phenylalanine, and methionine revealed variations of 0.9–14% for dopamine and 1–10% for uric acid (Table S1).

Conclusions

We developed a cost-efficient and facile method of fabricating a highly sensitive disposable electrode for the simultaneous detection of dopamine and uric acid. High sensitivity and selectivity were achieved in the modified electrode by introducing alternating layers of Au NPs and graphene. The improvement in the electrode sensitivity after modification indicated that the wrinkled graphene oxide and Au(III) GPE surface was reduced. All electrode fabrication parameters were optimized to obtain the best possible response for the simultaneous measurement of dopamine and uric acid. The linear range for dopamine and uric acid detection was identified. The LOQ and LOD were lower than or comparable to the corresponding values reported previously for graphene-based electrodes. The advanced electrochemical sensor provided good recovery of dopamine and uric acid in a human urine sample. The sensor displayed excellent sensitivity and selectivity, and good electrocatalytic activity and reproducibility. The disposable, cost-effectiveness, and rapid modification process distinguishes this electrode from other electrodes used to determine dopamine and uric acid.

Acknowledgements

The authors would like to acknowledge the support received from King Fahd University of Petroleum and Minerals (KFUPM) through Project No. SB141010.

References

- 1 M. Li, W. Guo, H. Li, W. Dai and B. Yang, *Sensors Actuators B Chem.*, 2014, **204**, 629–636.
- 2 T. E. M. Nancy and V. A. Kumary, *Electrochim. Acta*, 2014, **133**, 233–240.
- 3 L. Yang, D. Liu, J. Huang and T. You, *Sensors Actuators B Chem.*, 2014, **193**, 166–172.
- 4 H. Zhang, Q. Huang, Y. Huang, F. Li, W. Zhang, C. Wei, J. Chen, P. Dai, L. Huang, Z. Huang, L. Kang, S. Hu and A. Hao, *Electrochim. Acta*, 2014, **142**, 125–131.

- 5 B. Yang, H. Wang, J. Du, Y. Fu, P. Yang and Y. Du, *Colloids Surfaces A Physicochem. Eng. Asp.*, 2014, **456**, 146–152.
- 6 Z. Temoçin, *Sensors Actuators B Chem.*, 2013, **176**, 796–802.
- 7 P. Kalimuthu and S. A. John, *Bioelectrochemistry*, 2009, **77**, 13–18.
- 8 C. Wang, J. Du, H. Wang, C. Zou, F. Jiang, P. Yang and Y. Du, *Sensors Actuators B Chem.*, 2014, **204**, 302–309.
- 9 Z.-H. Sheng, X.-Q. Zheng, J.-Y. Xu, W.-J. Bao, F.-B. Wang and X.-H. Xia, *Biosens. Bioelectron.*, 2012, **34**, 125–131.
- 10 A. A. Ensafi, M. Taei and T. Khayamian, *J. Electroanal. Chem.*, 2009, **633**, 212–220.
- 11 X. Zhang, W. Yan, J. Zhang, Y. Li, W. Tang and Q. Xu, *RSC Adv.*, 2015, **5**, 65532–65539.
- 12 X. Zheng, Y. Guo, J. Zheng, X. Zhou, Q. Li and R. Lin, *Sensors Actuators B Chem.*, 2015, **213**, 188–194.
- 13 K. Ghanbari and N. Hajheidari, *Anal. Biochem.*, 2015, **473**, 53–62.
- 14 B. Kaur, B. Satpati and R. Srivastava, *New J. Chem.*, 2015, **39**, 1115–1124.
- 15 C. Wang, R. Yuan, Y. Chai, S. Chen, F. Hu and M. Zhang, *Anal. Chim. Acta*, 2012, **741**, 15–20.
- 16 Y. Shao, J. Wang, H. Wu, J. Liu, I. A. Aksay and Y. Lin, *Electroanalysis*, 2010, **22**, 1027–1036.
- 17 Y. Liu, X. Dong and P. Chen, *Chem. Soc. Rev.*, 2012, **41**, 2283–2307.
- 18 S. Wu, Q. He, C. Tan, Y. Wang and H. Zhang, *Small*, 2013, **9**, 1160–1172.
- 19 Y. J. Yang, *Sensors Actuators B Chem.*, 2015, **221**, 750–759.

- 20 Y. J. Yang and W. Li, *Biosens. Bioelectron.*, 2014, **56**, 300–306.
- 21 X. Tian, C. Cheng, H. Yuan, J. Du, D. Xiao, S. Xie and M. M. F. Choi, *Talanta*, 2012, **93**, 79–85.
- 22 J. Du, R. Yue, F. Ren, Z. Yao, F. Jiang, P. Yang and Y. Du, *Gold Bull.*, 2013, **46**, 137–144.
- 23 M. Abdul Aziz and A. N. Kawde, *Talanta*, 2013, **115**, 214–221.
- 24 N. Baig and A.-N. Kawde, *Anal. Methods*, 2015, **7**, 9535–9541.
- 25 T. Ndlovu, O. A. Arotiba, S. Sampath, R. W. Krause and B. B. Mamba, *Int. J. Electrochem. Sci.*, 2012, **7**, 9441–9453.
- 26 S. Ge, F. Lan, F. Yu and J. Yu, *New J. Chem.*, 2015, **39**, 2380–2395.
- 27 A. A. Abdelwahab and Y.-B. Shim, *Sensors Actuators B Chem.*, 2015, **221**, 659–665.
- 28 S. Wang, W. Zhang, X. Zhong, Y. Chai and R. Yuan, *Anal. Methods*, 2015, **7**, 1471–1477.
- 29 H. Han, D. Pan, X. Wu, Q. Zhang and H. Zhang, *J Mater Sci.*, 2014, **49**, 4796–4806.
- 30 J. Yan, S. Liu, Z. Zhang, G. He, P. Zhou, H. Liang, L. Tian, X. Zhou and H. Jiang, *Colloids Surf. B. Biointerfaces*, 2013, **111**, 392–397.
- 31 K. Deng, J. Zhou and X. Li, *Electrochim. Acta*, 2013, **114**, 341–346.
- 32 L. Zhao, H. Li, S. Gao, M. Li, S. Xu, C. Li, W. Guo, C. Qu and B. Yang, *Electrochim. Acta*, 2015, **168**, 191–198.
- 33 S. Li, Y. Wang, S. Hsiao, W. Liao, C. Lin, S. Yang, H. Tien, C. M. Ma and C. Hu, *J. Mater. Chem. C*, 2015, **3**, 9444–9453.
- 34 B. Kaur, T. Pandiyan, B. Satpati and R. Srivastava, *Colloids Surf. B. Biointerfaces*, 2013, **111**, 97–106.

- 35 Q. Lian, Z. He, Q. He, A. Luo, K. Yan, D. Zhang, X. Lu and X. Zhou, *Anal. Chim. Acta*, 2014, **823**, 32–39.

Table 1 Comparison of the fabricated electrochemical sensor with previously reported graphene modified sensors^a

Sr#	Electrodes	Analyte	Technique	Medium/pH	Linear range (μM)	LOQ (μM)	LOD (μM)	Peak separation (mV)	Ref.
1	Au/RGO/GCE	DA UA	DPV	0.1M PBS/ 7.0	6.8 – 41, 8.8 – 53	6.8 8.8	1.4 1.8	110	8
2	GE/Au/GE/CFE	DA UA	DPV	0.1M PBS/7.0	0.59 – 43.96, 12.6 – 413.62	0.59 12.6	0.59 12.6	-	22
3	AuNPs/β- CD/GR/GCE	DA UA	SWV	0.10 M NaH ₂ PO ₄ - HCl/2.0	0.5 – 150, 0.5 – 60	0.5 0.5	0.15 0.21	120	21
4	AuNCs/AGR/MW CNT/GCE	DA UA	SWV	0.1 M PBS/7.0	1.0 – 210, 5.0 – 100	1 5	0.08 0.1	140	27
5	RGO/PAMAM/M WCNT/AuNP/GCE	DA UA	DPV	0.1 M PBS/4.0	10 – 320, 1 – 114	10 1	3.3 0.33	120	28
6	rGO/MB/AuNPs/G CE	DA UA	DPV	PBS/7.4	–	-	0.15 0.25	132	29
7	Pd ₃ Pt ₁ /PDDA- RGO/GCE	DA UA	DPV	0.1 M PBS/7.4	4 – 200, 4 – 400	4 4	0.04 0.1	116	30
8	CoTPP- CRGO/GCE	DA UA	DPV	0.1 M PBS/6.5	0.1 – 12, 0.5 – 40	0.1 0.5	0.03 0.15	140	31
9	MgO/Gr/TaE	DA UA	DPV	0.1 M PBS/5.0	0.1 – 7, 1 – 70	0.1 1	0.15 0.12	147	32
10	CTAB- GO/MWCNT/GCE	DA UA	DPV	0.1 M PBS/7.0	5 – 500, 3 – 60	5 3	1.5 1.0	70	20
11	AgNW/rGO/SPCEs	DA UA	LSV	0.1 M PBS/7.4	40 – 450, 35 – 300	40 35	0.26 0.30	125	33
12	AgNPs/rGO/GCE	DA UA	LSV	PB/3.5	10 – 800, 10 – 800	10 10	5.4 8.2	124	34
13	Trp-GR/GCE	DA UA	DPV	0.1 M PBS/7.0	0.5 – 110, 10 – 1000	0.5 10	0.29 1.24	120	35
14	CTAB/rGO/ZnS/G CE	DA UA	DPV	0.1 M PB/7.0	1 – 500, 1 – 500	1 1	0.5 0.4	100	19
15	GR/Au/GR/Au/GP E	DA UA	SWV	0.1 M PBS/6.0	0.1 – 25, 0.09 – 25	0.1 0.09	0.024 0.029	151	This work

a Au/RGO/GCE: Au nanoplates/reduced graphene oxide/modified glassy carbon electrode; GE/Au/GE/CFE: graphene sheets/gold nanoparticles/carbon fiber electrode; AuNPs/β-CD/GR/GCE: β-cyclodextrin/graphene/GCE; AuNCs/AGR/MWCNT/GCE: gold nanoclusters/activated graphene/multiwall carbon nanotubes/GCE; RGO/PAMAM/MWCNT/AuNP/GCE: RGO/ poly(amido-amine)/MWCNT/AuNP/GCE; rGO/MB/AuNPs/GCE: reduced graphene oxide/methylene blue/AuNPs/GCE; Pd₃Pt₁/PDDA-RGO/GCE: Palladium–platinum bimetallic nanoparticles/ poly(diallyldimethylammonium

chloride)-RGO/GCE; CoTPP-CRGO/GCE: cobalt tetraphenylporphyrin- chemically reduced graphene oxide/GCE; MgO/Gr/TaE: MgO nanobelts/ graphene/tantalum wire electrode; CTAB-GO/MWCNT/GCE: hexadecyltrimethylammoniumbromide-GO/MWCNT/GCE; AgNW/rGO/SPCEs: Silver nanowire/rGO/ screen-printed carbon electrodes; Trp-GR/GCE: tryptophan-functionalized graphene/GCE; CTAB/rGO/ZnS/GCE: CTAB/rGO/zinc sulfide/GCE. NiCo-NPs-in-N/C modified GCE: Nickel cobalt alloy nanocrystal in N- doped carbon nanoplates modified GCE; PL-LEU/DNA/GCE: poly(L-leucine)/DNA/GCE; ZnO–Cu_xO–PPy/GCE: zinc oxide copper oxide/ polypyrrole/GCE; NiCo₂O₄/Nano-ZSM-5/GCE: NiCo₂O₄/ Nano crystalline zeolite/GCE; GNPs/PIlox/GCE: gold nanoparticles/ overoxidized polyimidazole/GCE.

Table 2 Determination of dopamine and uric acid in the human urine sample

Analyte	Found (μM)	Added (μM)	Recovered (μM)	Recovery (%)	RSD
Dopamine					
	0	2	2.18	109	8.08
	0	4	3.71	93	1.54
	0	8	7.48	93.5	5.54
Uric acid					
	4	2	1.88	94.1	5.55
	4	4	4.07	101	4.11
	4	8	7.76	97	3.37

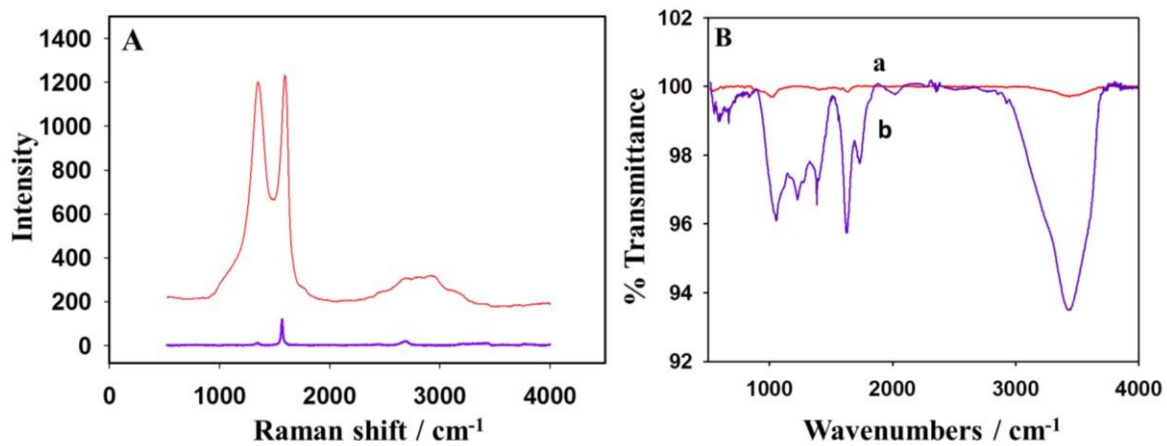


Fig. 1. (A) Raman spectra of graphite (a) and graphene oxide (b); (B) FTIR spectra of graphite (a) and graphene oxide (b).

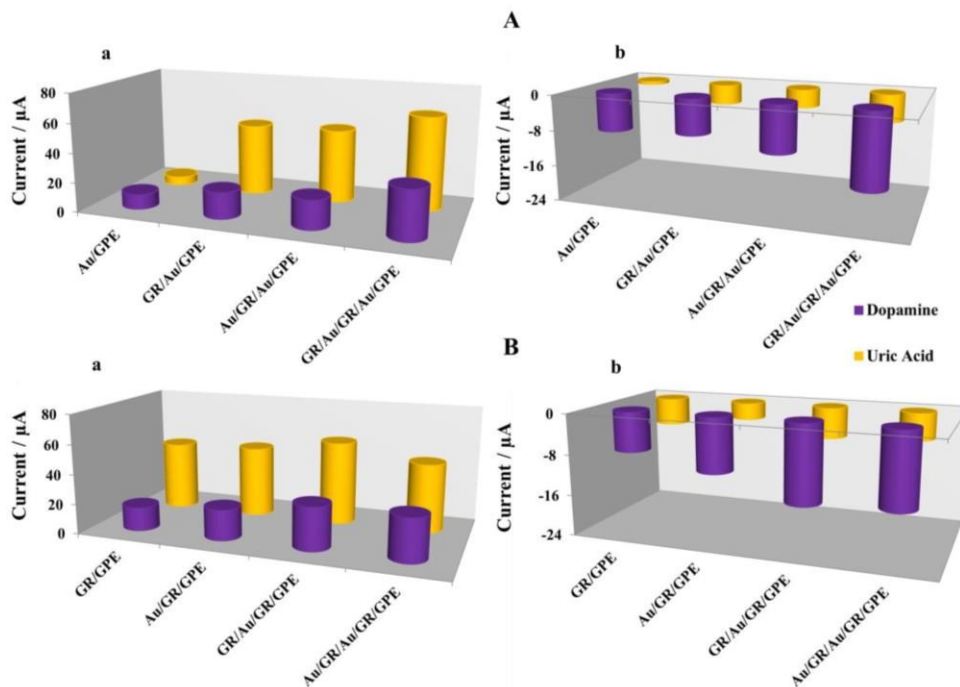


Fig. 2. Oxidizing (a) and reducing peak currents (b) obtained during collection of the 0.2 mM dopamine and uric acid cyclic voltammograms, for a starting layer of the Au NPs (A) or graphene (B) on the GPE surface.

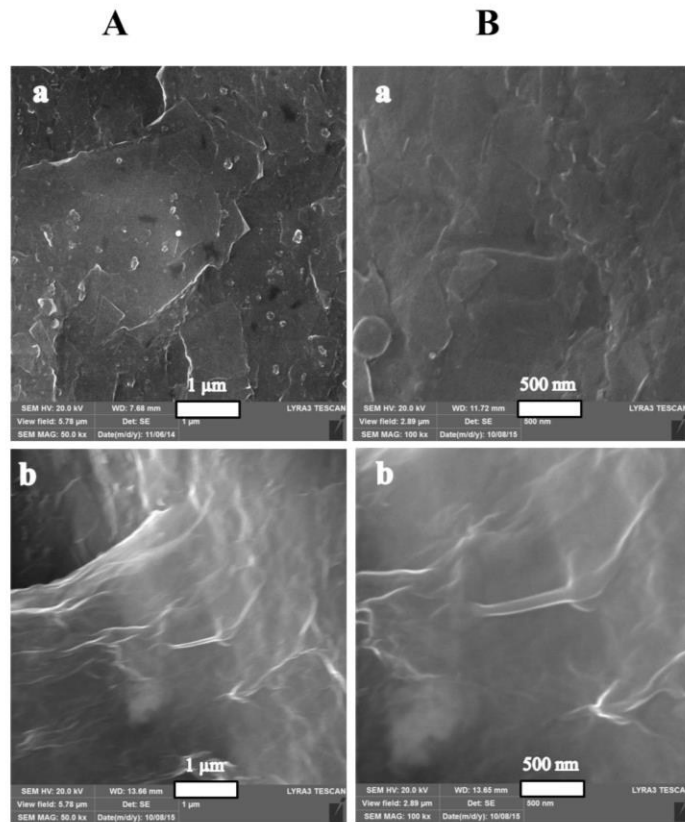


Fig. 3. FE-SEM images of the bare (a) and GR-GPE (b) at 1 μm (A) and 500 nm (B).

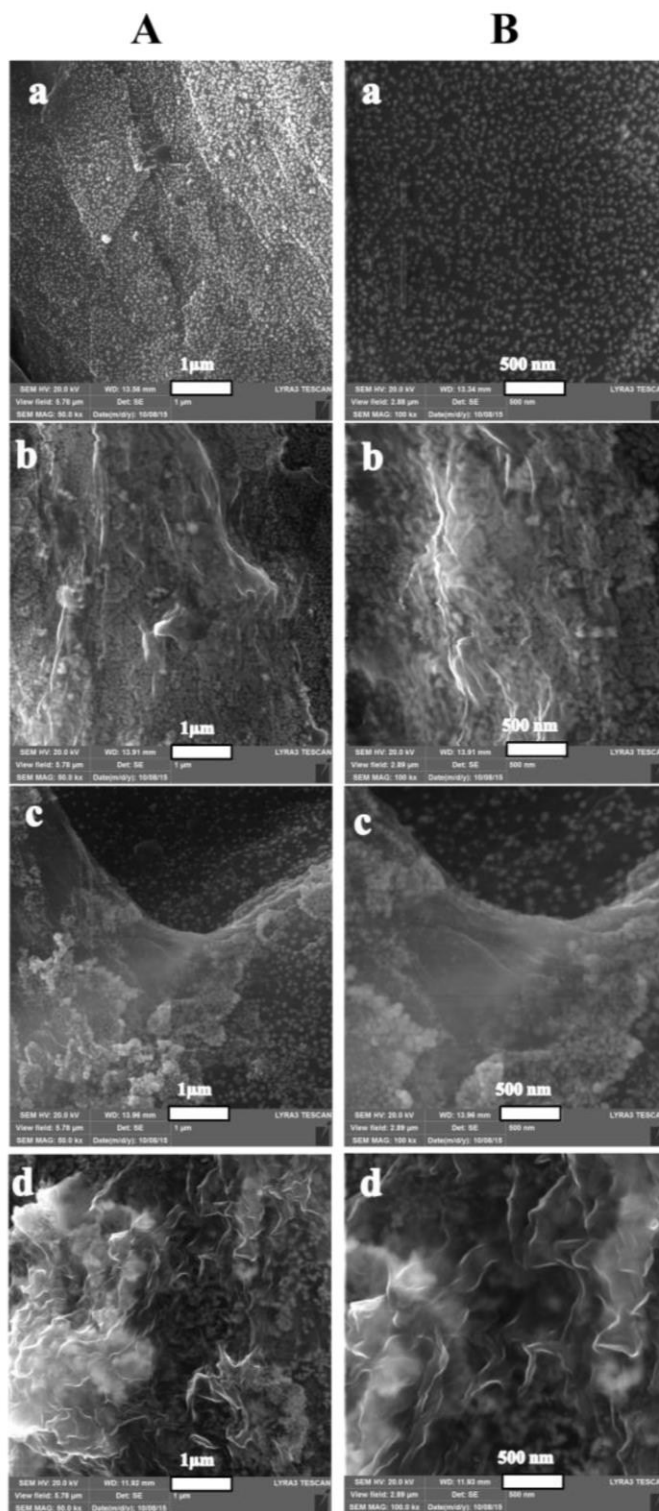


Fig. 4. FE-SEM images collected at two magnification values: 1 μm (A) or 500 nm (B), for the Au/GPE (a), GR/Au/GPE (b), Au/GR/Au/GPE (c), and GR/Au/GR/Au/GPE (d).

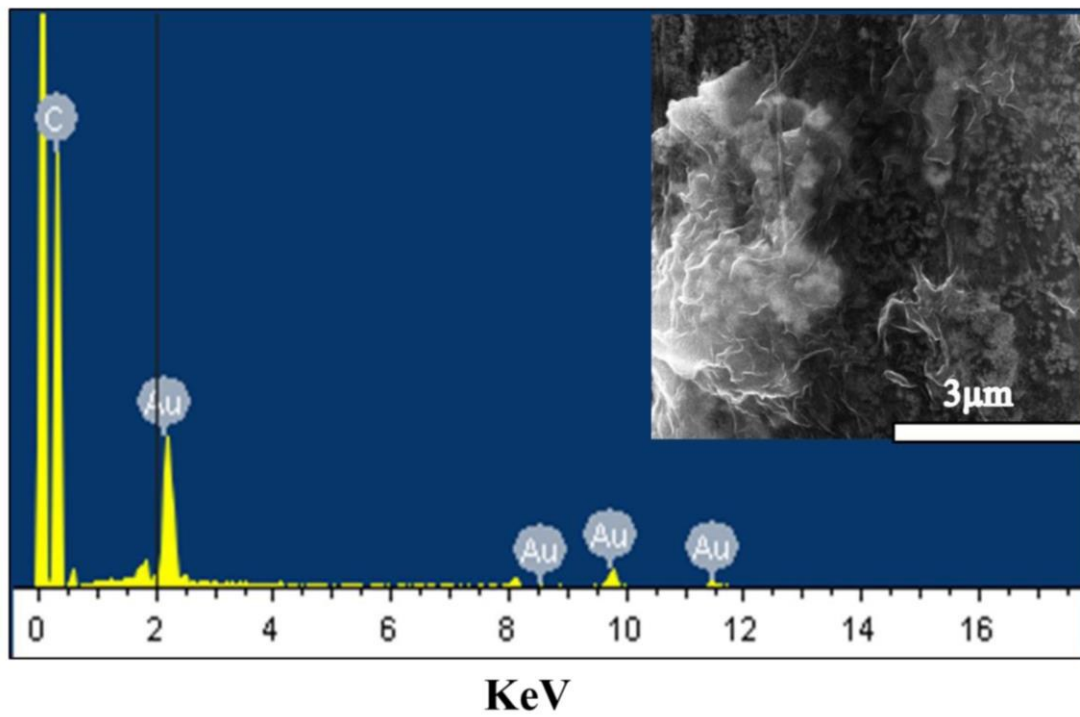


Fig. 5. EDX spectrum obtained from the GR/Au/GR/Au/GPE electrode.

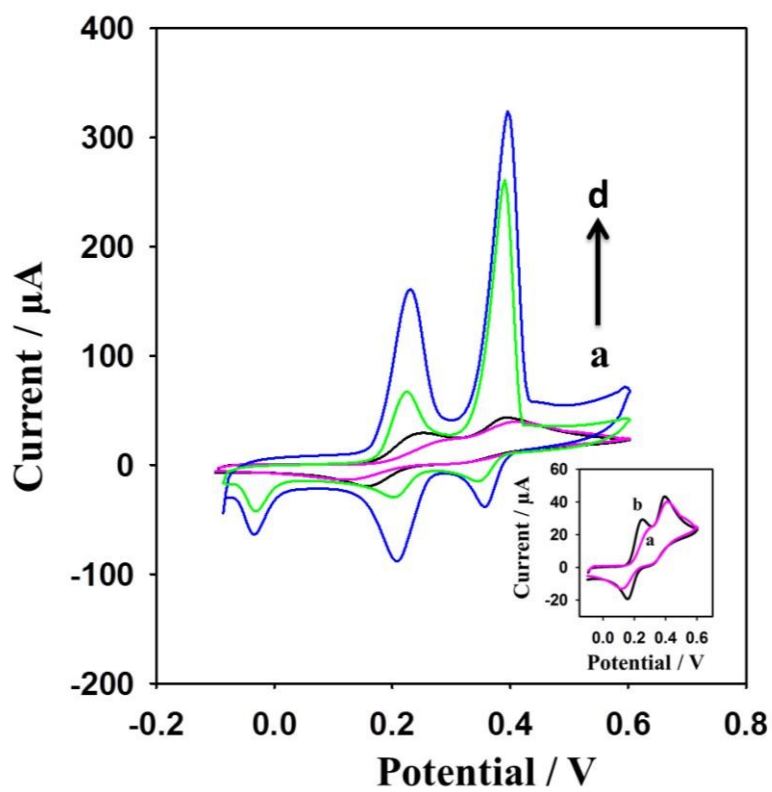


Fig. 6. Cyclic voltammograms of the bare GPE (a), Au NPs/GPE (b), GR/GPE (c), and GR/Au/GR/Au/GPE (d) in 0.1 M PBS containing 0.5 mM dopamine and uric acid.

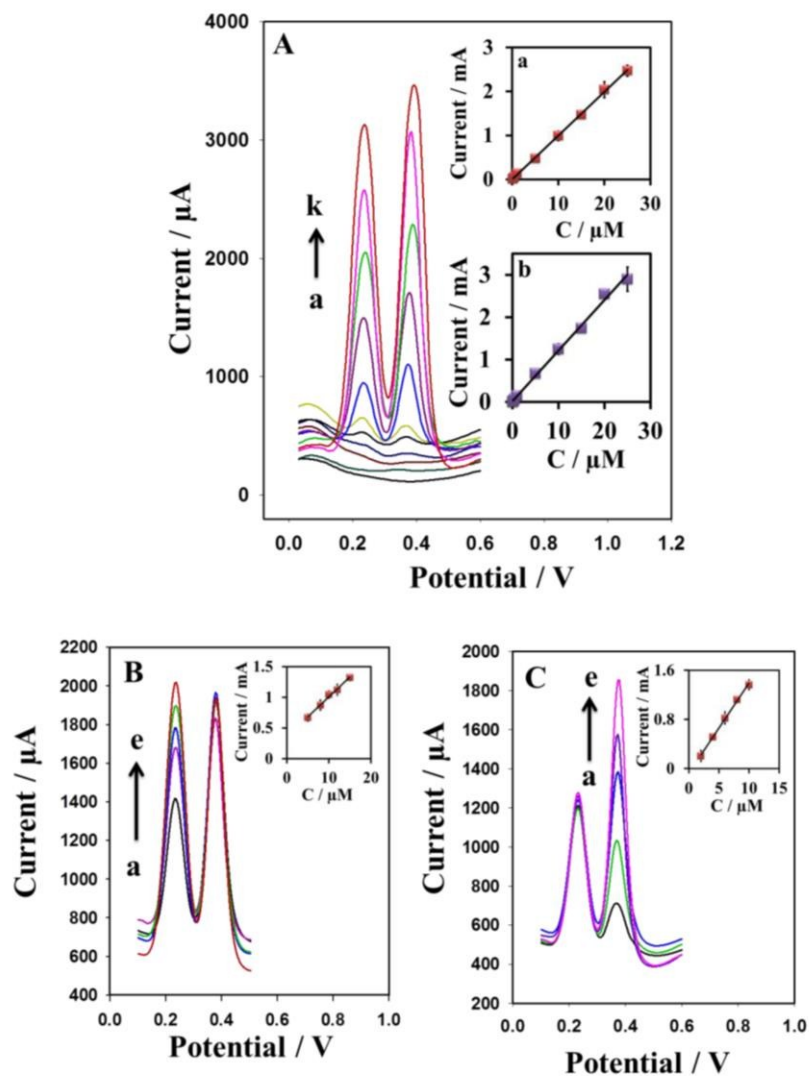
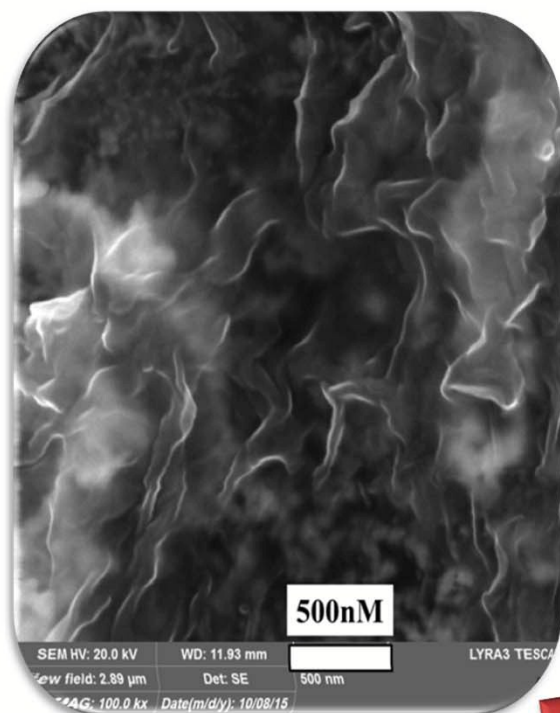
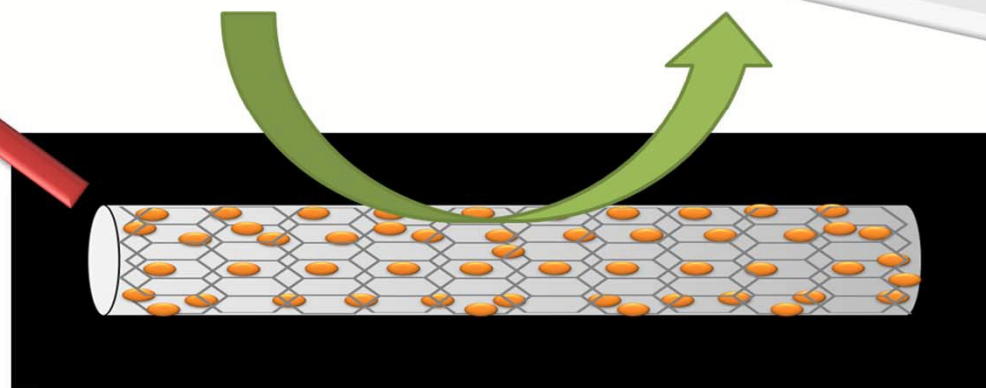
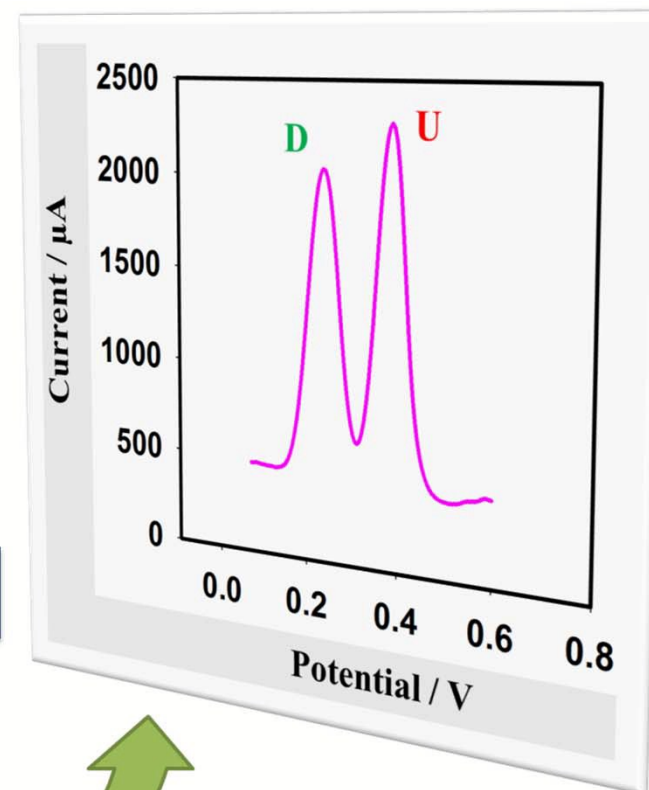


Fig. 7. Square wave voltammograms of (A) dopamine and uric acid at various concentrations: (a) 0 μM , (b) 0.09 μM , (c) 0.1 μM , (d) 0.3 μM , (e) 0.5 μM , (f) 1 μM , (g) 5 μM , (h) 10 μM , (i) 15 μM , (j) 20 μM , and (k) 25 μM . The inset shows the linear relationship between I (μA) and the concentration. (B) Dopamine concentrations: (a) 5 μM , (b) 8 μM , (c) 10 μM , (d) 12 μM , (e) 15 μM in the presence of 8 μM uric acid. (C) Uric acid concentrations: (a) 2 μM , (b) 4 μM , (c) 6 μM , (d) 8 μM , (e) 10 μM in the presence of 5 μM dopamine. The inset shows the linear relationship between I (μA) and the concentration (μM).



SEM Image

Uric acid + dopamine



Graphene-AuNP Modified GPE